Received: 3 April 2022 | Revised: 10 September 2022 | Accepted: 11 October 2022

DOI: 10.4218/etrij.2022-0130

ORIGINAL ARTICLE

ETRI Journal WILEY

Long range-based low-power wireless sensor node

Komal Devi | **Rita Mahajan** | **Deepak Bagai**

Electronics and Communication Engineering, Punjab Engineering College (Deemed to be University), Chandigarh, India

Correspondence
Komal Devi, Electronics and Communication Engineering, Punjab Engineering College (Deemed to be University), Chandigarh, India.
Email: komaldevi.phd19ece@pec.edu.in

Abstract

Sensor nodes are the most significant part of a wireless sensor network that offers a powerful combination of sensing, processing, and communication. One major challenge while designing a sensor node is power consumption, as sensor nodes are generally battery-operated. In this study, we proposed the design of a low-power, long range-based wireless sensor node with flexibility, a compact size, and energy efficiency. Furthermore, we improved power performance by adopting an efficient hardware design and proper component selection. The Nano Power Timer Integrated Circuit is used for power management, as it consumes nanoamps of current, resulting in improved battery life. The proposed design achieves an off-time current of 38.17309 nA, which is tiny compared with the design discussed in the existing literature. Battery life is estimated for spreading factors (SFs), ranging from SF7 to SF12. The achieved battery life is 2.54 years for SF12 and 3.94 years for SF7. We present the analysis of current consumption and battery life. Sensor data, received signal strength indicator, and signal-to-noise ratio are visualized using the ThingSpeak network.

KEYWORDS
long range (LoRa), low power, sensor node, spreading factor (SF), timer

1 | INTRODUCTION

The role of the Internet of Things (IoT) in human activities has increased in recent decades. Technology increases the efficiency of people in their daily routines, making many previously difficult jobs easy to complete. The advancements in technology has mandated the development of intelligent personal assistants, which are mobile, autonomous, and software-based systems that can perform functions or offer services on behalf of humans [1]. Wireless sensor networks (WSNs) have various applications and present several issues to be resolved. Based on a survey used to identify an active research field for every challenge, several research opportunities exist in the WSN field [2].

Several technologies enable energy -efficient IoT. We discuss several IoT elements that require efficient energy utilization [3]. Lazarescu [4] presented the WSN design for environmental-monitoring IoT applications. When designing WSNs, important aspects, such as platform structure, flexibility, and reusability, should be considered at all levels. A sensor node (Figure 1) is the most basic unit of a WSN. Processing, communication, power, and sensor units are the four essential parts of a sensor node [5].

Sensor node design in WSNs is influenced by various challenges and constraints, including power consumption,

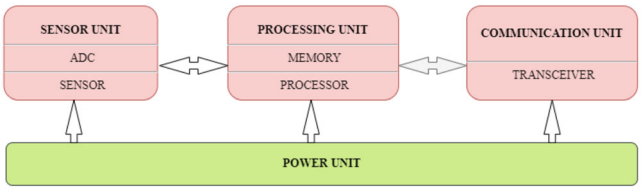

FIGURE 1 Basic components of sensor node

node deployment, hardware constraint, and security. As sensor nodes are usually battery operated, a major challenge in their design is power consumption. The batteries on power sensor nodes are recharged using diverse energy- harvesting (EH) techniques [6,7]. Various energy sources can be harvested, and various storage systems and existing EH sensor nodes exist. A hybrid EH system provides a sensor node for monitoring structural health. It detects the vibration, humidity, and temperature within the walls of the structure [8]. This sensor node is designed for specific use. Somov and others [9] first proposed power-aware gas sensing based on the principle of single-sensor gas concentration measurement. Previously, the Wheatstone bridge, composed of two sensors (one active and the other as a reference) and two resistors, was used for measurements.

1.1 | Related study

The green task-based sensing scheme (gTBS) is a cross-layer energy-efficient design that increases the lifespan of deployed sensor nodes and the overall WSN. It is a task-based sensing approach that incorporates power adaptability and a sleep-and-wake-up mechanism to allow idle nodes to sleep. A comparison was made between the power consumptions of the gTBS and the nongreen TBS with no energy-saving methods, and a reduction in power consumption was identified [10]. Yan and others [11] presented the design of an energy-aware sensor node. This architecture prioritizes energy conservation at the node and network levels. To save energy at the node-level, adaptive transmission power settings and a periodic sleep-and-wake-up system have been implemented. However, an adaptive network configuration is used to save energy at the network level. The software section provides a technique to determine the lowest possible output power.

Kumar and others [12] presented a design model for a smart sensing comfort system. The system was derived from a comfort rating technique based on WSNs. The system comprised a sensor array, a Simcom SIM20, a sink node, a central processing unit, and an SD card data storage module. The ATmega88 microcontroller was used as the processing unit, and Simcom SIM20 was used as a transceiver for designing this sensor node.

The authors proposed a two-antenna architecture for a power-efficient node. One antenna was for data transmission, although it was usually in sleep mode. The radio frequency (RF) signal sent to the node was detected using an additional antenna. The design included a wake-up circuit controlled by an RF power meter. The RF interface was activated when the power meter detected an RF signal. When data transmission was not required, the power consumption of the node was reduced. Compared with their previous work, the power reduction was around 21%, and compared with the standard node, it was almost 40% [13].

Magno and others [14] designed an ultra-low power, compact, and lightweight wireless sensor node for bird monitoring. Bluetooth Low Energy was employed for communication with this sensor node. ARM-Cortex M3 enabled bidirectional communication and minimized power consumption. Authors discussed the hardware implementation and design of ULP Long Range Wide Area Network (LoRaWAN) sensor node with sleep mode current consumption of 45 nA. The ATMEL SAM D21 low-power microcontroller, Murata CMWX1ZZABZ LoRa WAN modem (transceiver), and Ferroelectric random access memory (FRAM) were used to hold the keys and counters are used to design the sensor node [15]. Ali and others [16] proposed a WSN that operates independent of its location and orientation. Each side of the WSN unit was an EH wireless sensor module, incorporating a microprocessor, a RF transceiver, and an array of sensors. With the other faces, all sides shared a common energy storage unit and communication bus. The RF transceiver power consumption could be reduced using a directional antenna, and the most energy-efficient procedure for selecting the strongest radio face based on received signal strength indication (RSSI) was proposed. The Kalman filter and extended Kalman filtering methods were used to track the mobile nodes and predict their locations [17]. These techniques are used to reduce localization errors. It is found that the extended Kalman filtering approach is the best choice and was found to be optimal for monitoring the sensor nodes after assessing the received signal strength indication vs.RSSI against the distance for both filtering methods.

Pieris and others [18] presented different low-power strategies for constructing wireless sensor nodes. Linear voltage regulators were used in wireless sensor nodes to eliminate switching ripples and noise. However, voltage drops caused power consumption. Designing a sensor node without voltage regulators is one way to reduce power consumption, and this concept was used to create

a sensor node for saving energy. The nodes were designed using the BME280 sensor module for weather forecasting and the nRF24L01+ transceiver, which includes a built-in voltage regulator. Compared with the identical sensor node designed with a voltage regulator, this design saves up to 40% of the energy.

We present an overview of LoRaWAN, an open wireless communication standard. Furthermore, a power gradient approach has been developed to measure the power performance of the network. The lifetime and power gradient of an EH-based sensor node have also been estimated [19].

An application-based paper for groundwater monitoring was developed using long-range (LoRa) technology. The system built using the ATmega328P microprocessor uses the MS5803-14BA and MB280 sensors. Free and open-source software was used to develop the data processing, storage components, and data visualization dashboard [20]. The design of a new multipurpose, energy-efficient, adaptable, and low-cost sensor node has been described. The proposed sensor node has all the needed properties, including reconfigurability, flexibility, and energy efficiency. This sensor node enables the selection of a suitable communication module based on the desired communication range. The circuit design is presented to regulate the power consumption of various node parts to improve the lifespan of the sensor node. It can integrate peripherals to meet user needs [21]. This study describes a LoRa-based low-cost system with power management capabilities that contribute to increased battery life without reducing gateway communication time. The supercapacitor is an important component for supplying the required transmission. energy [22].

Most IoT sensor nodes are based on Zigbee, Bluetooth, and Wi-Fi communications. These methods have a restricted operating range and are inefficient for ultra-low-power sensor nodes. LoRa communication must be combined with ultra-low-power consumption and multiple-sensor interface support.

1.2 | Contribution

We proposed the design of a low-power, flexible, and compact-sized sensor node based on LoRa wireless technology for serving IoT applications. The design has an interface connector for communication with different sensors. A detailed analysis of current consumption and battery life is given. We took the initiative and proposed a low-power sensor node with the LoRa network. It achieves an off-time current in the nanoampere range that results in a long battery life. The values of the sensor are logged on the ThingSpeak channel. The channel displays temperature, humidity sensed by the sensor, RSSI, and signal-to-noise ratio (SNR). The contributions of our study are as follows:

- The proposed low-power LoRa-based wireless sensor node with a compact size achieves the off -time current in the nanoampere range.
- Analysis of the current consumption and battery life of the sensor node.
- Visualization of the sensor data and performance parameters, such as RSSI and SNR, on the ThingSpeak network.

2 | DESCRIPTION OF THE DIFFERENT UNITS OF THE PROPOSED SENSOR NODE

This section gives the basic idea of each unit used in the design of the sensor node. The main components of the proposed sensor node are the transceiver module unit and the timer unit. Figure 2 shows the components used for the hardware design of the sensor node.

2.1 | Processing unit

The processing unit is responsible for the different tasks, data processing and control of the different components. A PIC 18 family microcontroller PIC118LF46K22, the inbuilt part of the transceiver module, is the processing unit of the sensor node. This controller has an extremely low- power feature, as it consumes a 20-nA sleep current. It operates from 1.8 V to 3.6 V with up to 35 I/O pins, an Inter-Integrated Circuit (I2C), a Serial Peripheral Interface (SPI), a Timer/Counter, and a pulse-width modulation [23].

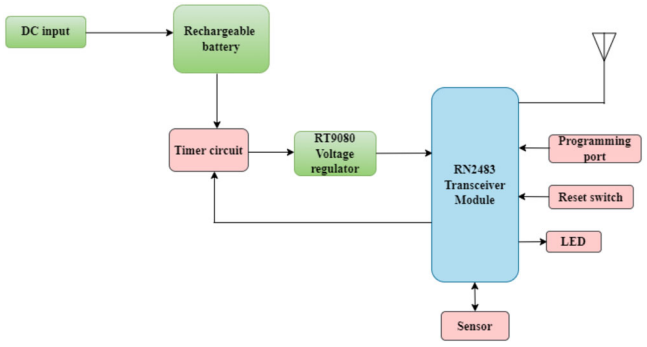

FIGURE 2 Components used for the hardware design of the sensor node

2.2 | Memory unit

The memory unit is an integral part of the transceiver chip used in the design. The internal memory of the inbuilt controller is 1024 bytes of electrically erasable programmable read-only memory (EEPROM), 64 Kbytes of linear program memory addressing, and 3896 bytes of linear data memory addressing. The executable files produced by the programmer are stored in the flash memory to serve the apps. The observed data are temporarily stored in an EEPROM (1 KB).

2.3 | Power unit

The power unit supplies power to the hardware of the sensor node. The onboard connector connects the power unit, comprising a 18650-type rechargeable battery attached to the top cover of the enclosure.

2.4 | Communication unit

The RN2483 transceiver module is the communication unit responsible for receiving and transmitting signals to and from the sensor nodes. It allows frequency-shift keying (FSK) modulation for a bitrate of up to 300 kbps, and the LoRa technology modulation provides a bitrate of 10 937 bps.

2.5 | Sensor unit

The sensor unit is an essential part of a wireless sensor node because it collects real-world data and sends it to the processing unit. There are 14 general-purpose input/outputs (GPIOs) available on the module, allowing different sensors to interface with the sensor node. This sensor node allows the connection of sensors compatible with various communication protocols, including SPI and I2C. The data acquisition section is built using a DHT11 sensor that can measure temperature and humidity, and the sense pin is connected with the GPIO10 of the module [24].

3 | DESIGN AND FUNCTIONALITY OF SENSOR NODE

This section discusses the hardware design and functionality of the proposed low-power LoRa-based sensor node. This design is adaptable because interfacing connectors are given on the board so that any GPIO can interface with any type of sensor. No GPIO is dedicated to a specific sensor.

3.1 | Circuit design

The schematic and PCB layout of the sensor node is designed in KiCad using KiCad 5.1.9. The circuit detail of each component is shown below.

3.1.1 | Timer module

This module is specifically used for the power management of the sensor node. The Nano Power Timer IC can operate at voltages ranging from 1.8 V to 5.5 V and currents of up to 1.1 amps. The onboard two-pin battery connector provides power. The circuit design of the timer module is shown in Figure 3.

The primary function of the Nano Power Timer IC is to turn on the transceiver module of the sensor node after a set time interval. The board has six dual in-line package switches that control this time by changing the resistance connected to the delay pin of the timer IC. The approximate time is labeled to the left of each switch. On the timer IC's output, a single white power light-emitting diode (LED) indicates the power supply to the voltage regulator input and enables pins. Simply disconnecting the trace between the jumper on the board disconnects this LED.

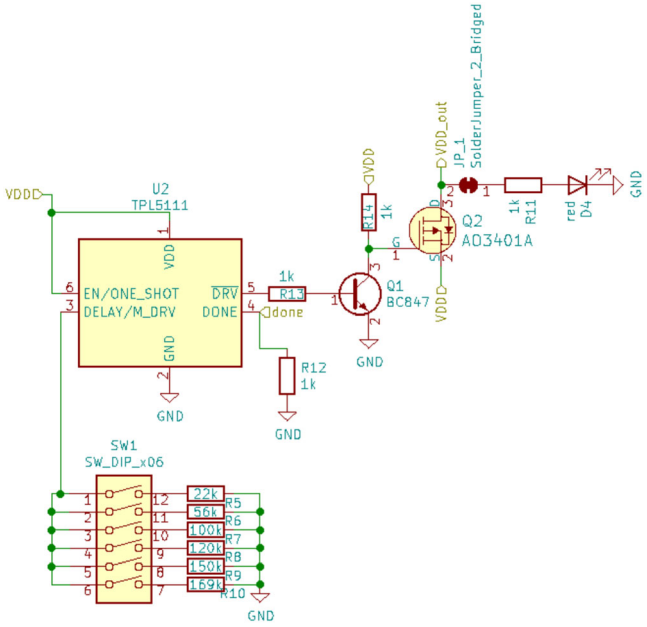

FIGURE 3 Components used for the design of the timer module

The GPIO-0 of the module provides a digital signal to the timer's done pin, which changes from low to high, and gives the off signal to the Nano Power Timer [25]. A pull-down resistor is connected to the done pin [26]. The Nano Power Timer will only consume 35 nA of current until the timer turns the main module back on again. The current consumption is significantly less than the sleep current of controllers used in designing other sensor nodes.

3.1.2 | LoRa module

Figure 4 shows the LoRa module unit of the sensor node and the circuit connections with an antenna connector, a programming port, an LED, a reset switch, and an interfacing connector.

The module provides the LoRa with high interference immunity. Some key attributes of the module are a single operating voltage from 2.1 V to 3.6 V (3.3 V typical), an integrated microcontroller unit (MCU), low-power consumption, FSK, Gaussian frequency-shift keying, LoRa technology modulation, and 14 GPIOs [27].

The output of the RT9080 voltage regulator supplies 3.3 V to the RN2483 LoRa module.

The radio transceiver is a LoRaWAN Class A protocol stack-based LoRaWAN technology radio that provides LoRa communication. The module has two RF signal pins, one for the high band, 868 MHz, and the other for the low band, 433 MHz. The antenna connector on the board is connected to the high-band RF signal. The programming connector has five pins connected to the internal MCU program clock, the internal MCU program data, the supplied 3.3 V, the ground, and the reset pin of the module. The LED is connected using a jumper at the GPIO-11 pin of the RN2483 module used in debugging while programming. The jumper can be disconnected after properly testing the sensor node due to the low-power requirement of the design. The reset switch is activated using a tactile push-button switch on the sensor node board.

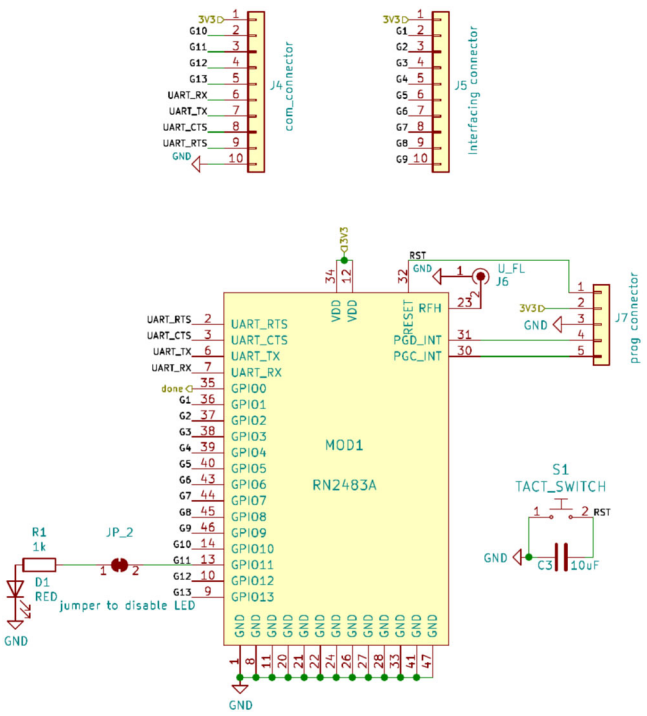

FIGURE 4 Connections of LoRa module with an antenna connector, a programming port, an LED, a reset switch, and an interfacing connector

3.1.3 | Voltage regulator

The voltage regulator RT9080 converts the voltage obtained from the timer circuit to the operating voltage required by the RN2483 module [28]. This regulator is selected because of its lower quotient current, 2 μA, compared with the voltage regulators used in the design of sensor nodes in related work.

3.2 | Software development

MPLAB X IDE v5.15 is used as the software environment to realize the LoRa MAC protocol RN2483 LoRaWAN v1.00 from library name RN2483 [29]. The node is programmed using the PIC Kit 3.5 programmer. The sensor node uses an Activation by Personalization scheme in The Things Network (TTN). We stored the LoRaWAN session keys and frame counter values in the internal EEPROM of the microcontroller.

3.3 | Functionality

The front view of the proposed sensor node, housed in a waterproof enclosure, is shown in Figure 5.

The temperature sensor is attached outside the enclosure for temperature and humidity sensing. A LoRa antenna of 2.6-dBi gain and an 868-MHz frequency is mounted on the other side of the enclosure, and a battery is attached to the lid. The sensor node transmits data depending on the switch selected on the board. The switch determines the time interval after which the RN2483 transceiver module is turned on.

Six switches on the board select the different time intervals from approximately 1 min to 2 h. Table 1 can be used to determine an approximate time based on the switch pressed on the board with the resistance value.

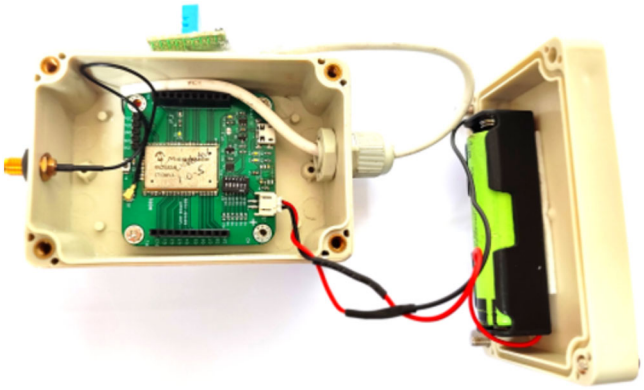

FIGURE 5 Proposed sensor node in ABS enclosure

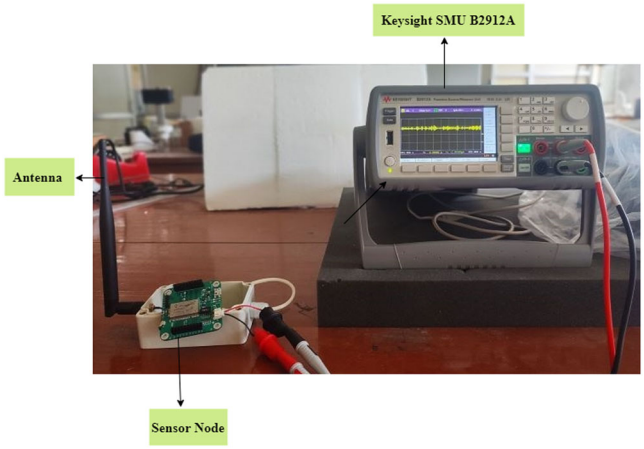

FIGURE 6 Experimental setup for the current consumption analysis

TABLE 1 List of available timer values

Timer	Switch	Resistance
2 h	1	169 kΩ
1.5 h	2	150 kΩ
1 h	3	120 kΩ
35 min	4	100 kΩ
10 min	5	56 kΩ
1 min	6	22 kΩ

The time depends on the value of the resistors connected to the switches, and the other end of each resistor is connected to the delay pin of the timer IC.

4 | EXPERIMENTAL EVALUATION AND RESULT ANALYSIS

4.1 | Performance parameters

4.1.1 | Current consumption analysis

A highly accurate B2912A source measure unit used to measure the current and experimental setup to analyze the current of the sensor node is shown in Figure 6.

The average current used by the sensor node is evaluated during the on- and off-time frames. The current is calculated as follows:

$$I = I_{\text{on}} + I_{\text{off}}\,, \tag{1}$$

$$I_{on} = I_{\text{init}} + I_{\text{sensor}} + I_{\text{trans}} + I_{\text{save}}. \tag{2}$$

Here, I_{init}, I_{sensor}, I_{trans}, and I_{save} denote the current consumed for system initialization, sensor data acquisition and processing, LoRa transmission, and information storage, respectively.

4.1.2 | Battery life

We estimated the battery life that powers the sensor node. The battery life L_{lt} is estimated by dividing the capacity rating of the battery in mWh by the total average power consumed by the sensor node and power consumption because of the self - discharge rate. The steps used to estimate the lifetime are as follows:

$$L_{\text{lt}} = (\text{Cap}_{\text{bat}}^{\text{tot}}/P_{\text{avg}} + P_{\text{sd}})/24. \tag{3}$$

Here, $\text{Cap}_{\text{bat}}^{\text{tot}}$, P_{avg}, and P_{sd} denote the total power capacity of the battery, the average power consumed by the sensor node, and the power consumed due to self-discharge in mWh, respectively.

$$\text{Cap}_{\text{bat}}^{\text{tot}} = V_b \cdot C_{\text{bat}}. \tag{4}$$

Here, V_b and C_{bat} denote the nominal battery voltage and battery capacity in mAh, respectively.

$$P_{\text{avg}} = V \cdot I_{\text{avg}}. \tag{5}$$

Here, V and I_{avg} denote the operational voltage and average current consumed by the sensor node in mAh, respectively.

$$I_{\text{avg}} = (I_{\text{on}}^{\text{avg}} + I_{\text{off}}^{\text{avg}}). \tag{6}$$

Here, $I_{\text{on}}^{\text{avg}}$ and $I_{\text{off}}^{\text{avg}}$ denote the average current consumption during on and off times.

$$I_{\text{on}}^{\text{avg}} = DC_{\text{on}} \cdot I_{\text{on}}. \tag{7}$$

Here, DC_{on} indicates the on-time duty cycle, and I_{on} is the on-time current consumed by the sensor node.

$$DC_{on} = T_{on}^{day} / T_{sec}^{day}. \quad (8)$$

Here, T_{on}^{day} and T_{sec}^{day} denote the on time in a day and the total seconds in a day, respectively.

$$T_{on}^{day} = N_{on} \cdot t_{on} \cdot 24. \quad (9)$$

Here, N_{on} and t_{on} denote the number of on times per hour and the duration of the on time, respectively.

The on-time frame includes different cycles: System-initialized time (t_{init}), sensor data acquisition and processing time (t_{sensor}), LoRa transmission time (t_{trans}), and LoRa information save time (t_{save}). Table 2 gives the details of the required transmission time for different spreading factors (SFs). The payload size is 5 bytes, and the transmission time value is verified for each SF, according to the formula given in Petrariu and others [22]

$$t_{on} = t_{init} + t_{sensor} + t_{trans} + t_{save}, \quad (10)$$

$$I_{off}^{avg} = (1 - DC_{on}) \cdot I_{off}. \quad (11)$$

Here, I_{off} is the off-time current consumed by the sensor node.

$$P_{sd} = V_b \cdot I_{sd}. \quad (12)$$

Here, I_{sd} is the approximate average current consumed due to the self-discharge of the battery.

TABLE 2 Transmission time of each SF

Spreading factor (SF)	Transmission time (ms)
SF7	40.4
SF8	76.0
SF9	121.2
SF10	283.0
SF11	499.0
SF12	824.0

4.2 | Results

4.2.1 | Current consumption

The nominal battery voltage V_b is 3.7. Figure 7 shows the actual value of the current consumed for various SFs, ranging from SF7 to SF12. The total on-time current consumption is calculated by taking the average current

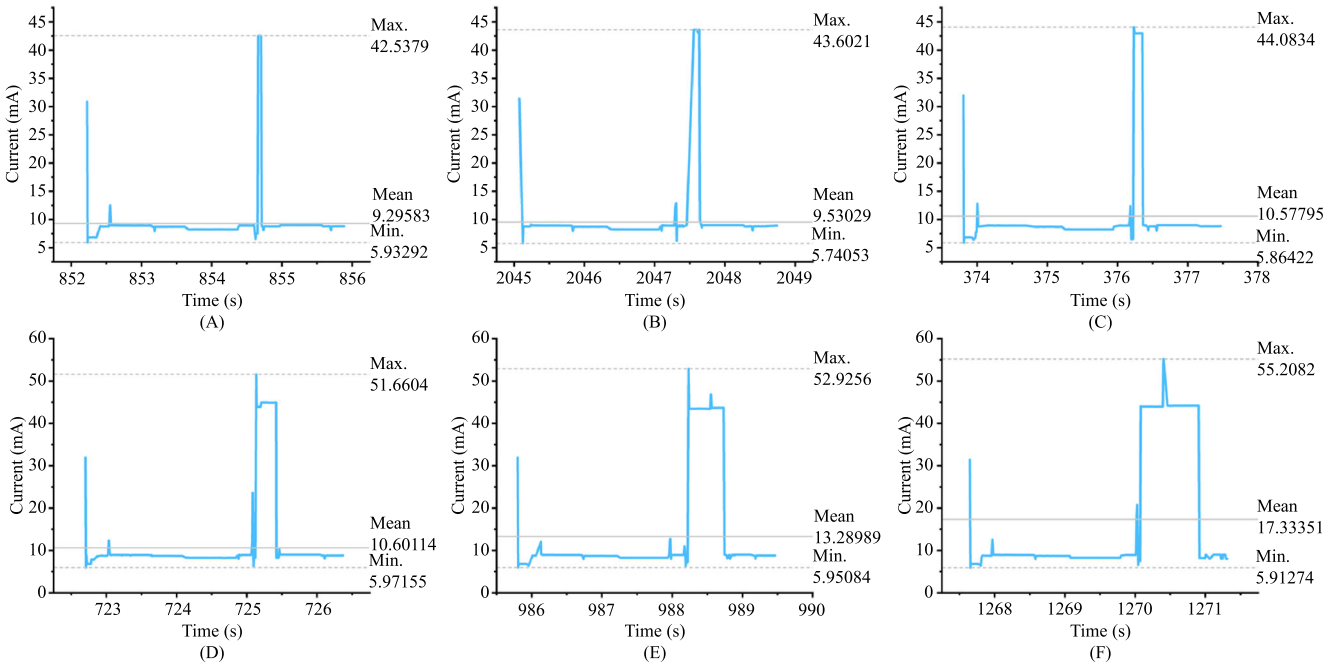

FIGURE 7 Current consumption during on time (A) SF7, (B) SF8, (C) SF9, (D) SF10, (E) SF11, and (F) SF12

consumed within the on-time period. The minimum, maximum, and mean values of the current are shown in the graph for each SF. An average value is used in the battery life calculation. Table 3 gives the measured value of the on-time current for various SFs, ranging from SF7 to SF12.

The graphical and table views depict that the on-time current consumption of the sensor node is at the maximum when SF12 is used. Figure 8 represents the graph of off-time current.

The average current during the off time is in the nanoampere range, which is much lower than that of the sensor nodes mentioned in related studies. This is due to the proper component selection used in the efficient hardware design of the node. Table 4 shows the comparison of the off-time current.

TABLE 3 Average current consumption of nodes during on time

Spreading factor (SF)	On -time current (mA)
SF7	9.296
SF8	9.531
SF9	10.578
SF10	10.601
SF11	13.289
SF12	17.334

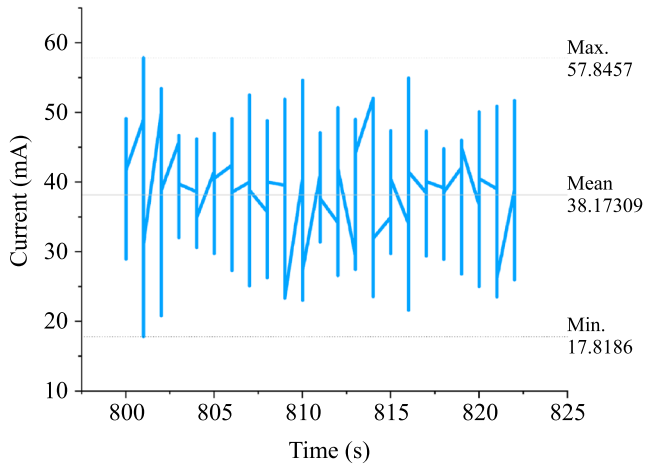

FIGURE 8 Graphical view of current consumption during off time

TABLE 4 Comparison of the off -time current

current consumption	Proposed	Asenov and Tokmakov [15]
Off -time current (nA)	38.17309	45

The table above shows that the proposed sensor node design achieved less current in the off mode than the previous paper based on a low-power timer.

4.2.2 | Battery Life

We consider the N_{on} as equal to 0.5 because the timer turns the main module on every 2 h, and the value of t_{on} is 3.67 s. A self-discharge rate of 0.75% is considered for the battery life evaluation. The battery lifetime L_{lt} is evaluated for various SFs and compared with the lifetime of the sensor node proposed in Petrariu and others [22]. The same battery capacity (230 mAh) is used to calculate the L_{lt} for comparison with the battery life calculated in Petrariu and others [22].

Figure 9 depicts the battery life comparison graph. The battery life is shown to decrease with an increased SF because current consumption is higher in the higher SF. The battery life is always longer in days compared

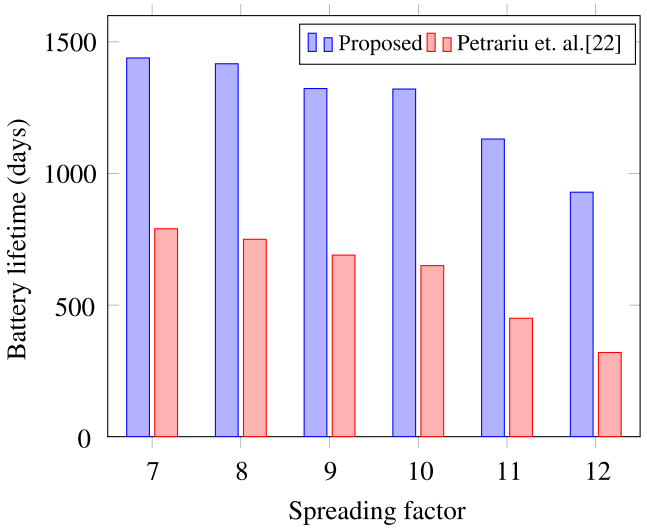

FIGURE 9 Battery life comparison with that of Petrariu et al. [22]

TABLE 5 Battery life comparison

SF	Proposed	Petrariu et al. [22]
7	1439	790
8	1417	750
9	1323	690
10	1321	650
11	1131	450
12	929	320

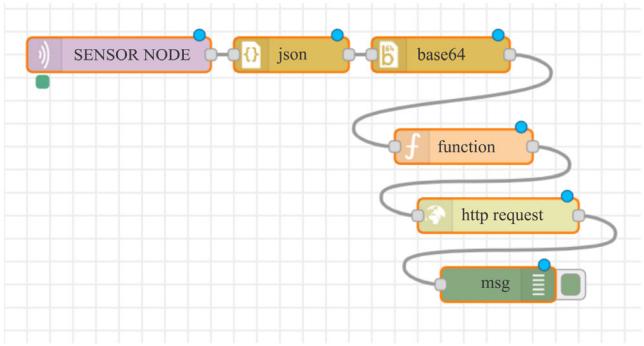

FIGURE 10 Flow created in Node-RED

with the battery life calculated in the paper [22]. Table 5 gives the battery life comparison.

4.3 | Visualization

The sensor node collects temperature and humidity data, which are then sent to an application over TTN. A data log is required to display the temperature, humidity, and RSSI of sensor nodes. However, data cannot be stored on TTN. For storage and viewing, data must be transferred to another network server. ThingSpeak receives data from TTN's Message Queue Telemetry Transport (MQTT) integration through Node-RED. Node-RED is a flow-based visual programming tool for developing IoT. Figure 10 shows the flow designed to deliver data from TTN to ThingSpeak. avaScript Object Notation (JSON) stores the flows made in Node-RED.

The sensor node is called "connects to an MQTT broker." The broker's internet protocol address or name, as well as the port, must be known to connect to an MQTT broker or server. TTN provides the information needed for this node [30]. This node receives messages from the specified topic and subscribes to them. The body of the message will be stored in the msg.payload property.

The ThingSpeak link is given in the function node, where the channel is created to represent temperature and relative humidity. This link can be used by anyone [31] to visualize the detailed view of these parameters.

One channel on the ThingSpeak network with four fields is created. Field 1 displays relative humidity, Field 2 displays the temperature obtained from the DHT11 sensor, Field 3 shows the RSSI value, and Field 4 shows the SNR. The HTTP request node is the network node for sending JSON data to ThingSpeak. The HTTP node will send a request and receive the response. The debug node displays messages and informs viewers when the message was sent and received.

5 | CONCLUSION

We presented the hardware of a low-power LoRa-based wireless sensor node that is adaptable and small. The dimension of the developed sensor node PCB is 53 mm × 55 mm. The timer circuit controls the activation of the whole circuit depending on the switch selection on the board. All the hardware components are carefully selected so that they can reduce the current consumption of the proposed sensor node when data transmission is not required. We concluded that the proposed approach provides an off-time current of 38.17309 nA, which is considerably lower than that of the existing sensor nodes presented in related work. Such a small average current value during off time is not possible with the deep sleep feature of microcontrollers. We proposed a hardware design with a low-power timer to turn the hardware on and off with a sleep current in nanoamps. This is one of the most significant contributions to the design of an energy-efficient sensor node. We achieved a 15.17% off-time current reduction over the previous timer-based sensor node.

CONFLICT OF INTEREST

The authors declare that there are no conflicts of interest.

ORCID

Komal Devi https://orcid.org/0000-0002-7720-7638

REFERENCES

1. J. Santos, J. J. P. C. Rodrigues, J. Casal, K. Saleem, and V. Denisov, *Intelligent personal assistants based on internet of things approaches*, IEEE Syst. J. **12** (2018), no. 2, 1793–1802.
2. S. P. Singh and S. C. Sharma, *A survey on research issues in wireless sensor networks*, Open Trans. Wirel. Sensor Netw. **2** (2015), no. 1, 1–18.
3. F. K. Shaikh, S. Zeadally, and E. Exposito, *Enabling technologies for green Internet of Things*, IEEE Syst. J. **11** (2017), no. 2, 983–994.
4. M. T. Lazarescu, *Design of a WSN platform for long-term environmental monitoring for Iot applications*, IEEE J. Emerg. Sel. Top. Circ. Syst. **3** (2013), no. 1, 45–54.
5. L. Cui, F. Wang, H. Luo, H. Ju, et al., *A pervasive sensor node architecture*, (IFIP International Conference on Network and Parallel Computing, Whnam, China), 2004, pp. 565–567.
6. O. B. Akan, O. Cetinkaya, C. Koca, and M. Ozger, *Internet of hybrid energy harvesting things*, IEEE Internet Things J. **5** (2018), no. 2, 736–746.
7. S. Sudevalayam and P. Kulkarni, *Energy harvesting sensor nodes: Survey and implications*, IEEE Commun. Surv. Tutor. **13** (2011), no. 3, 443–461.
8. S. Siddheswar, S. Biplab, and D. Uma, *Design of wireless sensor node to measure vibration and environment parameter for structural health monitoring application*, *Intelligent computing and applications*, Springer, 2015, pp. 59–65.

9. A. Somov, A. Baranov, D. Spirjakin, and R. Passerone, *Circuit design and power consumption analysis of wireless gas sensor nodes: One-sensor versus two-sensor approach*, IEEE Sensors J. **14** (2014), no. 6, 2056–2063.
10. A. Alhalafi, L. Sboui, R. Naous, and B. Shihada, *gTBS: A green task-based sensing for energy efficient wireless sensor networks*, (IEEE Conference on Computer Communications Workshops, San Francisco, CA, USA), 2016, pp. 136–143.
11. R. Yan, H. Sun, and Y. Qian, *Energy-aware sensor node design with its application in wireless sensor networks*, IEEE Trans. Instr. Meas. **62** (2013), no. 5, 1183–1191.
12. A. Kumar and G. P. Hancke, *An energy-efficient smart comfort sensing system based on the IEEE 1451 standard for green buildings*, IEEE Sensors J. **14** (2014), no. 12, 4245–4252.
13. L. Catarinucci, S. Guglielmi, R. Colella, and L. Tarricone, *Pattern-reconfigurable antennas and smart wake-up circuits to decrease power consumption in WSN nodes*, IEEE Sensors J. **14** (2014), no. 12, 4323–4324.
14. M. Magno, F. Vultier, B. Szebedy, H. Yamahachi, R. H. R. Hahnloser, and L. Benini, *A Bluetooth-low-energy sensor node for acoustic monitoring of small birds*, IEEE Sensors J. **20** (2020), no. 1, 425–433.
15. S. M. Asenov and D. M. Tokmakov, *Development of Ultra-Low Power Sensor Node Using FRAM and Nano Timer*, 2020. https://doi.org/10.1109/electronica50406.2020.9305121
16. K. Ali and D. J. Rogers, *An orientation-independent multi-input energy harvesting wireless sensor node*, IEEE Trans. Ind. Electr. **68** (2021), no. 2, 1665–1674.
17. M. Sunitha and R. K. Karunavathi, *Localization of nodes in underwater wireless sensor networks*, (4th International Conference on Recent Trends on Electronics, Information, Communication & Technology, Bangalore, India) 2019, pp. 820–823.
18. T. P. D. Pieris, K. V. D. S. Chathuranga, A. L. Kulasekera, P. Guha, and P. Mukhija, *Energy and power consumption analysis of a wireless sensor node without a voltage regulator*, (5th International Conference on Information Technology Research, (Moratuwa, Sri Lanka), 2020, pp. 1–6.
19. N. Dinh, Tveito, and Haugen, *Performance evaluation for energy harvesting (EH)-based sensor nodes under Lorawan connectivity*, (IEEE Eighth International Conference on Communications and Electronics, Phu Quoc Island, Vietnam), 2021, pp. 64–69.
20. O. H. Kombo, S. Kumaran, and A. Bovim, *Design and application of a low-cost, low-power, LoRa-GSM, IoT enabled system for monitoring of groundwater resources with energy harvesting integration*, IEEE Access **9** (2021), 128417–128433.
21. S. Misra, S. K. Roy, A. Roy, M. S. Obaidat, and A. Jha, *MEGAN: multipurpose energy-efficient, adaptable, and low-cost wireless sensor node for the Internet of Things*, IEEE Syst. J. **14** (2020), no. 1, 144–151.
22. A. I. Petrariu, A. Lavric, E. Coca, and V. Popa, *Hybrid power management system for LoRa communication using renewable energy*, IEEE Internet Things J. **8** (2021), no. 10, 8423–8436.
23. PIC18(L)F2X/4XK22. Low-Power, *High-Performance Microcontrollers with nanoWatt XLP Technology Datasheet*. https://pdf1.alldatasheet.com/datasheet-pdf/view/348768/MICROCHIP/PIC18LF46K22.html, [Online; accessed on: Oct. 25, 2021].
24. DHT11, *Humidity and Temperature Sensor Datasheet*. https://www.mouser.com/datasheet/2/758/DHT11-Technical-Data-Sheet-Translated-Version-1143054.pdf, [Online; accessed on: Nov. 17, 2021].
25. TPL5111, *Nano-Power System Timer for Power Gating Datasheet*. https://datasheetspdf.com/pdf-file/1411520/etcTI/TPL5111/1, [Online; accessed on: Dec. 14, 2021].
26. *Timer module reference for done pin*. https://learn.sparkfun.com/tutorials/tpl5110-nano-power-timer-hookup-guide/all#resources-and-going-further, [Online; accessed on: Dec. 12, 2021].
27. RN2483, *Transceiver Module Datasheet*. http://ww1.microchip.com/downloads/en/devicedoc/50002346c.pdf, [Online; accessed on: Sep. 9, 2021].
28. RT9080, *Low-Dropout Linear Regulator Datasheet*. https://www.richtek.com/assets/product_file/RT9080/DS9080-00.pdf, [Online; accessed on: Jun. 14, 2021].
29. RN283 library. https://github.com/kamval/RN2483, [Online; accessed on: Dec. 10, 2021].
30. MQTT, *Steps for MQTT integration*. https://www.thethingsindustries.com/docs/integrations/mqtt/, [Online; accessed on: Oct. 22, 2021].
31. ThingSpeak, *Public view of channel*. https://thingspeak.com/channels/1548502, [Online; accessed on: Nov. 14, 2021].

AUTHOR BIOGRAPHIES

Komal Devi received her BTech in Electronics and Communication Engineering from Kurukshetra University, Kurukshetra, Haryana, India, in 2011 and her MTech in Very Large-Scale Integration Design from Punjab Engineering College Chandigarh, India, in 2019. She is currently pursuing a PhD in Electronics and Communication Engineering from Punjab Engineering College Chandigarh, India. She has nearly 2 years of teaching experience. Her research interests include digital design, very large-scale integration design, embedded system design, Internet of Things applications, and wireless sensor networks.

Rita Mahajan from Thapar University, Patiala, Punjab, India, in 1986 and her MTech and PhD in Electronics Engineering from Punjab Engineering College, Chandigarh, India, in 1993 and 2016, respectively. She has 31 years of teaching experience. She is currently working as an assistant professor in the Electronics and Communication Engineering Department of Punjab Engineering College, Chandigarh, India. She has published more than 20 papers in national journals and conferences. Her research interests include digital design, very large-scale integration design, neural network communication systems, and cognitive radio networks.

Deepak Bagai received his BTech, MTech, and PhD in Electronics Engineering from Punjab Engineering College, Chandigarh, India, in 1985, 1992, and 1997, respectively. He has 34 years of teaching experience. He is currently working as a professor in the Electronics and Communication Engineering Department of Punjab Engineering College, Chandigarh, India. He has published more than 40 papers in national and international journals and conferences. His research interests include cognitive radio networks, communication systems, and wireless sensor networks.

How to cite this article: K. Devi, R. Mahajan, and D. Bagai, *Long range-based low-power wireless sensor node*, ETRI Journal **45** (2023), 570–580. https://doi.org/10.4218/etrij.2022-0130